

First PPMXL photometric analysis of open cluster Ruprecht 15

Ashraf Latif Tadross

National Research Institute of Astronomy & Geophysics, 11421-Helwan, Cairo, Egypt;
altadross@yahoo.com

Received 2011 September 8; accepted 2011 October 31

Abstract We present the first in a series studying the astrophysical parameters of open clusters using the PPMXL* database whose data are applied to study Ruprecht 15. The astrophysical parameters of Ruprecht 15 have been estimated for the first time.

Key words: open clusters and associations (individual: Ruprecht 15) — astrometry — stars — astronomical databases: catalogs

1 INTRODUCTION

This paper is a part of our continuing series whose goal is to obtain the main astrophysical properties of previously unstudied open clusters using modern databases. The most important aspect of using the PPMXL database lies in the positions and proper motions of USNO-B1.0¹ and the Near Infrared (NIR) photometry of the Two Micron All Sky Survey (2MASS)², respectively, which allow the powerful detection of star clusters behind the hydrogen thick clouds that are concentrated in the Galactic plane.

The only available information about Ruprecht 15 (hereafter Ru 15) is the coordinates and the optical apparent diameter, which were obtained from the WEBDA³ site and the last updated version of the DIAS⁴ collection (version 3.0, 2010 April 30). This cluster is located in the southern Milky Way at J2000.0 coordinates $\alpha = 07^{\text{h}}19^{\text{m}}34^{\text{s}}$, $\delta = -19^{\circ}37'30''$, $\ell = 233.54^{\circ}$, $b = -2.896^{\circ}$, and its diameter is about 2.0 arcmin. Figure 1 represents the blue image of Ru 15 taken from the Digitized Sky Survey (left panel), while the right panel shows the J -image of the cluster taken from the Interactive 2MASS Image Service⁵.

This paper is organized as follows. PPMXL data extraction is presented in Section 2, while data analysis and reduction for estimating parameters are described in Section 3. Finally, the conclusion is devoted to Section 4.

2 PPMXL DATA EXTRACTION

The current PPMXL Catalog of Roeser et al. (2010) combines the proper motion data of USNO-B1.0 and the NIR JHK_s pass-band of 2MASS databases. USNO-B1.0 of Monet et al. (2003) is a spatially

* <http://vizier.cfa.harvard.edu/viz-bin/VizieR?-source=I/317>

¹ <http://vizier.cfa.harvard.edu/viz-bin/VizieR?-source=I/284>

² <http://vizier.cfa.harvard.edu/viz-bin/VizieR?-source=II/246>

³ <http://obswww.unige.ch/webda>

⁴ <http://www.astro.iag.usp.br/~wilton/>

⁵ <http://irsa.ipac.caltech.edu/applications/2MASS/IM/interactive.html>

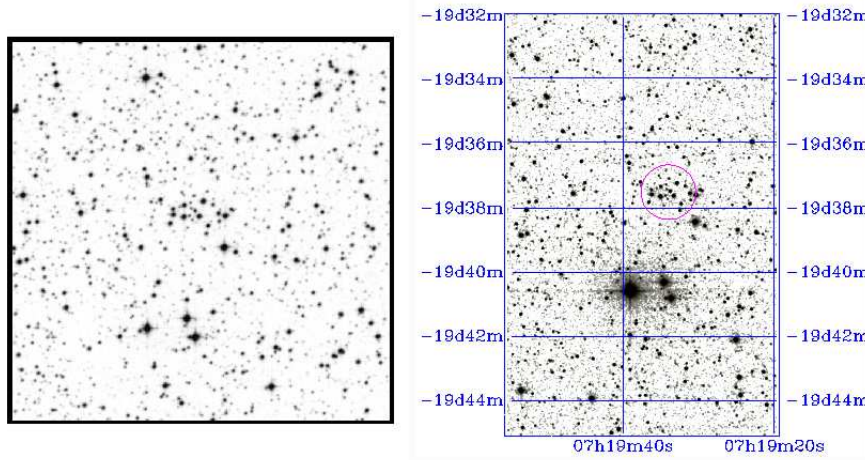


Fig. 1 Left panel represents the blue image of Ru 15 taken from the Digitized Sky Surveys, while the right panel represents the J -image of the cluster taken from the Interactive 2MASS Image Service. The small open circle indicates the cluster's central part. North is up, east on the left.

unlimited catalog that presents positions, proper motions and magnitudes in various optical passbands. The data were obtained from scans of Schmidt plates taken for the various sky surveys during the last 50 years. USNO-B is believed to provide all-sky coverage, with completeness down to $V = 21$ mag. It is noted that, based on the proper motion measurements, stars with large proper motions are likely to be foreground stars instead of cluster members. Background stars cannot readily be distinguished from members by proper motions. Nonetheless, identifying foreground stars is useful in cleaning up the color-magnitude diagrams (CMDs) and determining the field star contamination. So, USNO-B is a very useful catalog, which gives us an opportunity to distinguish between the members and background/field stars.

On the other hand, the NIR 2MASS photometry provides some direct answers to questions on the large scale structure of the Milky Way and the local Universe. It provides J , H and K_s band photometry for millions of galaxies and nearly a half-billion stars (Carpenter 2001). 2MASS observations were obtained using two highly automated 1.3-m telescopes, one at Mount Hopkins in Arizona (northern survey) and the other at Cerro Tololo in Chile (southern survey). Each telescope was equipped with a three-channel camera, with each channel consisting of a 256×256 array of HgCdTe detectors. It uniformly scanned the entire sky in the three NIR bands J ($1.25 \mu\text{m}$), H ($1.65 \mu\text{m}$) and K_s ($2.17 \mu\text{m}$). This survey has proven to be a powerful tool in the analysis of the structure and stellar content of open clusters (Bica et al. 2003; Bonatto & Bica 2003). The photometric uncertainty of the 2MASS data is less than 0.155 at $K_s \sim 16.5$ magnitude which is the photometric completeness for stars with $|b| > 25^\circ$ (Skrutskie et al. 2006).

Ru 15 is located near the Galactic plane ($|b| < 3^\circ$), therefore we expect significant foreground and background field contamination. The apparent diameter is less than 5 arcmin, hence the downloaded data have been extended to the field background stars, where the cluster dissolves. We extracted the data to a radius of about 20 arcmin.

Each star has 3-color photometric values J , H , K_s mag; and proper motion (pm) values in right ascension (α) and declination (δ), i.e. (pm $\alpha \cos \delta$ & pm δ) mas yr $^{-1}$. According to Roeser et al. (2010), the stars with pm uncertainties ≥ 4.0 mas yr $^{-1}$ have been removed. In this context, to get a net worksheet of data for Ru 15, the photometric completeness limit has been applied on the

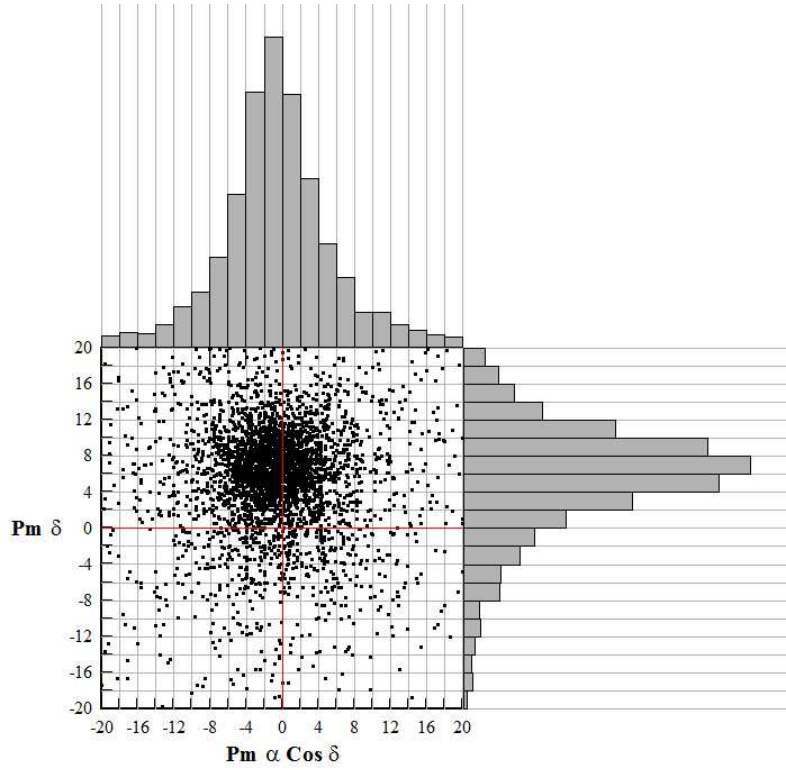


Fig. 2 Proper motion vector point diagram VPD of Ru 15 after avoiding all data with pm errors $\geq 4 \text{ mas yr}^{-1}$. Histograms of 2 mas yr^{-1} bins in both directions are drawn. The Gaussian function fit to the central bins provides the mean pm $\alpha \cos \delta = -0.84 \pm 0.1 \text{ mas yr}^{-1}$ and pm $\delta = 6.7 \pm 0.09 \text{ mas yr}^{-1}$.

photometric pass-band 2MASS data to avoid the over-sampling at the lower parts of the cluster's CMDs (cf. Bonatto et al. 2004). The stars with observational uncertainties $\geq 0.20 \text{ mag}$ have been removed (Claria & Lapasset 1986). A pm vector point diagram (VPD) with a distribution histogram of 2 mas yr^{-1} bins for $(\text{pm } \alpha \cos \delta)$ and $(\text{pm } \delta)$ has been constructed as shown in Figure 2. To filter the inner region of the VPD, the outer region, where field stars dominate, should be excluded. The radius of the inner region is in agreement with the cluster limited radius. The Gaussian function fit to the central bins provides the mean pm in both directions. All data lying in the region of the mean $\pm 1 \sigma$ (where σ is the standard deviation of the mean) can be considered as astrometric probable members. In addition, the stellar photometric membership criteria are adopted based on the location of the stars within $\pm 0.1 \text{ mag}$ around the zero age main sequence (ZAMS) curve in the CMDs.

3 DATA ANALYSIS AND REDUCTION

3.1 Cluster's Center and Radial Density Profile

The star-count method has been applied to the whole area of Ru 15, and the 20 arcmin data that were obtained around the adopted center are divided into equal sized bins in α and δ . The cluster

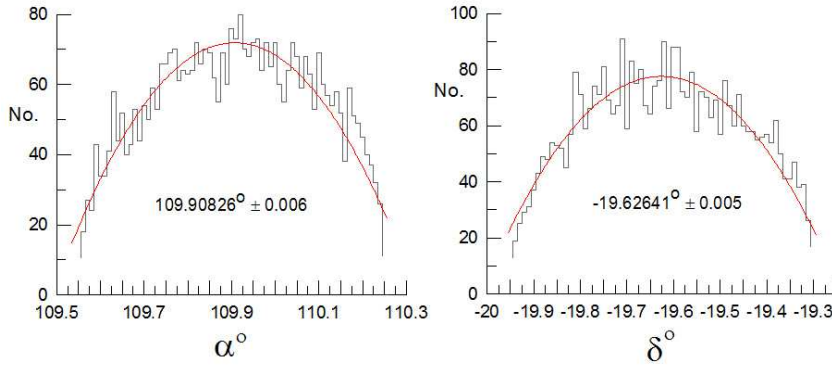


Fig. 3 An estimation of the cluster center coordinates of Ru 15. The Gaussian fit provides the coordinates of the highest density areas in α and δ as $07^{\text{h}}19^{\text{m}}38^{\text{s}}$ and $-19^{\circ}37'35''$ respectively. The differences between our estimated centers and the ones obtained from WEBDA are 4^{s} in α and $5''$ in δ .

center is defined as the location of maximum stellar density of the cluster's area. The two Gaussian curve-fittings are applied to the profiles of star counts in α and δ respectively as shown in Figure 3. The differences between our estimated centers and the ones obtained from WEBDA are shown in the figure.

To establish the radial density profile (RDP) of Ru 15, we counted the stars within concentric shells in equal incremental steps ($r \leq 1$ arcmin) from the cluster center. We repeated this process for $1 < r \leq 2$ up to $r \leq 10$ arcmin, i.e. the stellar density is derived out to the primary radius of the cluster. The star counts of the next steps would be subtracted from the previous ones, so that we obtained only the number of stars within the relevant shell's area, not a cumulative count. Finally, we divided the star counts in each shell by the area of that shell those stars belong to. The density uncertainties in each shell were calculated using Poisson noise statistics. Figure 4 shows the RDP from the new center of Ru 15 to the maximum angular separation of 5 arcmin where the density becomes stable. To determine the structural parameters of the cluster more precisely, we applied the empirical King model (King 1966). The King model parameterizes the density function $\rho(r)$ as

$$\rho(r) = f_{\text{bg}} + \frac{f_0}{1 + (r/r_c)^2}, \quad (1)$$

where f_{bg} , f_0 and r_c are background density, central star density and the core radius of the cluster respectively. From the concentration parameter c , defined as $c = (R_{\text{lim}}/R_{\text{core}})$, Nilakshi et al. (2002) concluded that the angular size of the coronal region is about six times the core radius. Maciejewski & Niedzielski (2007) reported that R_{lim} may vary for individual clusters between about $2R_{\text{core}}$ and $7R_{\text{core}}$. In our case, we can see that $R_{\text{lim}}=6.9R_{\text{core}}$, i.e. it agrees with the previous values. The cluster's limiting radius can be defined at that radius which covers the entire cluster area and reaches the stability of the background density, i.e. the difference between the observed density profile and the background one is almost equal zero. It is noted that the determination of a cluster radius is made by the spatial coverage and uniformity of PPMXL photometry which allows one to obtain reliable data on the projected distribution of stars for large extensions to the clusters' halos. On the other hand, the concentration parameter seems to be related to the cluster age, i.e. for clusters younger than about 1 Gyr, it tends to increase with the cluster age. Nilakshi et al. (2002) noted that the halos' sizes are smaller for older systems. Finally, we can infer that open clusters appear to be somewhat

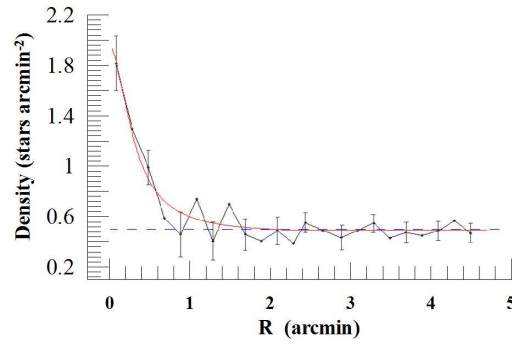


Fig. 4 Radial density distribution for stars in the field of Ru 15. The density shows a maximum at the center of $\rho = 63$ stars arcmin $^{-2}$ and then decreases down to $\rho = 3$ stars arcmin $^{-2}$ at 2.2 arcmin, where the decrease becomes asymptotical. The curved solid line represents the fitting of the King (1966) model. Errors bars are determined from sampling statistics ($1/\sqrt{N}$ where N is the number of stars used in the density estimation at that point). The dashed line represents the background field density, where $f_{bg} = 3.0$ stars arcmin $^{-2}$. The core radius $r_c = 0.32$ arcmin.

larger in the NIR than in the optical data (Sharma et al. 2006). Knowing the cluster’s total mass (Sect 3.3), the tidal radius can be given by applying the equation of Jeffries et al. (2001)

$$R_t = 1.46 (M_c)^{1/3} = 10.7 \text{ pc}, \quad (2)$$

where R_t and M_c are the tidal radius and total mass of the cluster respectively.

3.2 Color-Magnitude Diagrams

Using the 2MASS ZAMS solar metallicity isochrones of Marigo et al. (2008) and downloading isochrones⁶ from Padova, we obtain the photometrical parameters age, reddening and distance by applying several isochrones of different ages to both CMDs ($J, J - H$) and ($K_s, J - K_s$) of Ru 15. These fits should be obtained at the same distance modulus for both diagrams, and the color excesses should obey Fiorucci & Munari (2003)’s relations for a normal interstellar medium as shown in Figure 5.

The observed data have been corrected for interstellar reddening using the coefficient ratios $\frac{A_J}{A_V} = 0.276$ and $\frac{A_H}{A_V} = 0.176$, which were derived from absorption ratios in Schlegel et al. (1998), while the ratio $\frac{A_{K_s}}{A_V} = 0.118$ was derived from Dutra et al. (2002).

Fiorucci & Munari (2003) calculated the color excess values for the 2MASS photometric system. We ended up with the following results: $\frac{E_{J-H}}{E_{B-V}} = 0.309 \pm 0.130$, $\frac{E_{J-K_s}}{E_{B-V}} = 0.485 \pm 0.150$, where $R_V = \frac{A_V}{E_{B-V}} = 3.1$. Also, we can de-redden the distance modulus using these formulae: $\frac{A_J}{E_{B-V}} = 0.887$, $\frac{A_{K_s}}{E_{B-V}} = 0.322$, then the distance of the cluster from the Sun (R_\odot) can be calculated. Therefore, $(m - M)_J = 11.90 \pm 0.10$ mag ($\sim 1845 \pm 85$ pc), $E(J - H) = 0.20 \pm 0.05$ mag and $(J - K_s) = 0.31 \pm 0.07$ mag.

After estimating the cluster’s distance R_\odot , then the distance from the galactic center (R_g), the projected distances on the galactic plane from the Sun (X_\odot and Y_\odot), and also the distance from the galactic plane (Z_\odot) can be determined, see Table 1. For more details about the distance calculations, see Tadross (2011).

⁶ <http://stev.oapd.inaf.it/cgi-bin/cmd>

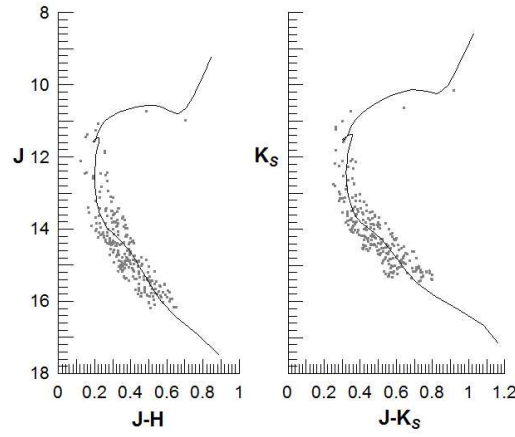


Fig. 5 Net NIR CMDs of Ru 15 for stars lying close to the fitted isochrones and after removing all contaminated field stars. Age = 500 Myr, distance modulus = 11.9 mag (~ 1845 pc), $E(J - H) = 0.20$ mag and $(J - K_s) = 0.31$ mag.

3.3 Luminosity, Mass Functions and the Total Mass

It is difficult to determine the membership of the cluster using only the stellar RDP. The stellar membership is found more precisely for those stars that are close to the cluster's center and at the same time very near to the main-sequence (MS) in CMDs. These MS stars are very important in determining the luminosity, mass functions (MFs) and the total mass of the investigated cluster.

The number of stars per luminosity interval, or in other words, the number of stars in each magnitude bin, gives us the so-called luminosity function (LF) of the cluster. In order to estimate the LF of Ru 15 we count the observed stars in terms of absolute magnitude after applying the distance modulus as shown in Figure 6. The magnitude bin intervals are selected to include a reasonable number of stars in each bin and for the best possible statistics of the luminosity and MFs. In this context, the total luminosity is found to be ~ -4.1 mag.

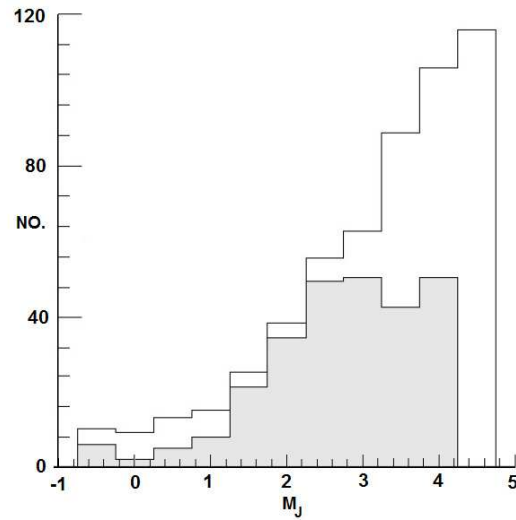
The LF and the MF are correlated to each other according to the known mass-luminosity relation. The accurate determination of both of them (LF and MF) suffers from some problems, e.g. the field contamination of the cluster members; the observed incompleteness of low-luminosity (or low-mass) stars; and mass segregation, which may affect even poorly populated, relatively young clusters (Scalo 1998). On the other hand, the properties and evolution of a star are closely related to its mass, so the determination of the initial mass function (IMF) is needed, which is an important diagnostic tool for studying large quantities of star clusters. An IMF is an empirical relation that describes the mass distribution (a histogram of stellar masses) of a population of stars in terms of their theoretical initial mass (the mass they were formed with). The IMF is defined in terms of a power law as

$$\frac{dN}{dM} \propto M^{-\alpha}, \quad (3)$$

where $\frac{dN}{dM}$ is the number of stars in mass interval ($M : M + dM$) and α is a dimensionless exponent. The IMF for massive stars ($> 1 M_{\odot}$) was studied and well established by Salpeter (1955), where $\alpha = 2.35$. The Salpeter form shows that the number of stars in each mass range decreases rapidly with increasing mass. It is noted that the cluster Ru 15 has an MF slope ranging around the Salpeter value as shown in Figure 7.

Table 1 Present Results of Ruprecht 15

Parameter	Present Result
Center	$\alpha = 07^{\text{h}} 19^{\text{m}} 38^{\text{s}}$ $\delta = -19^{\circ} 37' 35''$
c	6.9 (see Sect 3.1)
pm $\alpha \cos \delta$	$-0.84 \pm 0.10 \text{ mas yr}^{-1}$
pm δ	$6.7 \pm 0.09 \text{ mas yr}^{-1}$
Age	$500 \pm 60 \text{ Myr}$
Metal abundance	0.019
$E(J - H)$	$0.20 \pm 0.05 \text{ mag}$
$E(J - K_s)$	$0.31 \pm 0.07 \text{ mag}$
$E(B - V)$	$0.65 \pm 0.05 \text{ mag}$
R_V	3.1 (see Sect 3.2)
Distance Modulus	$11.90 \pm 0.10 \text{ mag}$
Distance	$1845 \pm 85 \text{ pc}$
R_{lim}	$2.2' (1.20 \text{ pc})$
Membership	265 stars
f_o	$63 \pm 2 \text{ stars arcmin}^{-2}$
f_{bg}	$3 \text{ stars arcmin}^{-2}$
R_c	$0.32' \pm 0.04 (0.20 \text{ pc})$
R_t	10.7 pc
R_g	9.7 kpc
X_{\odot}	1095 kpc
Y_{\odot}	-1482 kpc
Z_{\odot}	-93 pc
τ	> 100 (see Sect 3.4)
Total Luminosity	$\sim -4.1 \text{ mag}$
IMF slope	$\Gamma = -2.37 \pm 0.20$
Total mass	$\sim 390 M_{\odot}$
Relaxation time	2.7 Myr

**Fig. 6** Luminosity function of Ru 15 in terms of the absolute magnitude M_J . The color and magnitude filter cutoffs have been applied to the cluster (dark area) and the field (white area) respectively.

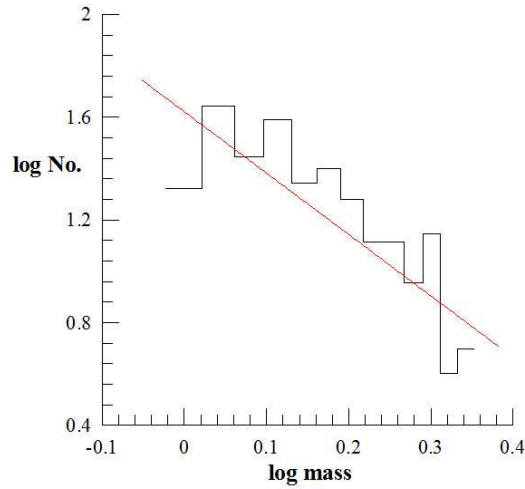


Fig. 7 Mass function of Ru 15. The slope of the IMF is found to be $\Gamma = -2.37 \pm 0.20$ with a correlation coefficient of 0.82.

To estimate the total mass of Ru 15, the mass of each star has been estimated from a polynomial equation developed from the data of the solar metallicity isochrones (absolute magnitudes vs. actual masses) at the age of the cluster (500 Myr). The summation of multiplying the number of stars in each bin by the mean mass of that bin yields the total mass of the cluster, which is about $390 M_{\odot}$.

3.4 Dynamical State and Relaxation Time

The time, in which the cluster needs from the very beginning to build itself to the moment when it reaches the stability state against the contraction and destruction forces, is known as the relaxation time (T_{relax}) of the cluster. T_{relax} mainly depends on the number of members and the cluster diameter. To describe the dynamical state of the cluster, the relaxation time can be calculated in the form

$$T_{\text{relax}} = \frac{N}{8 \ln N} T_{\text{cross}}, \quad (4)$$

where $T_{\text{cross}} = D/\sigma_V$ denotes the crossing time, N is the total number of stars in the investigated region of diameter D , and σ_V is the velocity dispersion (Binney & Tremaine 1987) with a typical value of 3 km s^{-1} (Binney & Merrifield 1998). Using the above formula we can estimate the dynamical relaxation time for Ru 15, and then the dynamical-evolution parameter τ can be calculated for the cluster by

$$\tau = \frac{\text{age}}{t_{\text{relax}}}, \quad (5)$$

If the cluster's age is found to be greater than its relaxation time, i.e. $\tau \gg 1.0$, then the cluster is dynamically relaxed, and vice versa. In our case, Ru 15 is indeed dynamically relaxed, where $\tau > 100$.

4 CONCLUSIONS

The astrophysical parameters of yet unstudied open cluster Ru 15 have been estimated using the PPMXL database. This cluster is found to have a real stellar density profile. Its stellar members are

lying at the same absolute distance modulus and reddening range. Its IMF slope is in agreement with the Salpeter (1955) value, and its age is greater than its relaxation time, which infers that this cluster is indeed dynamically relaxed. All the astrophysical parameters of Ru 15 are listed in Table 1.

Acknowledgements It is worth mentioning that this publication made use of the WEBDA and DIAS catalogs and the data products from the PPMXL database of Roeser et al. (2010).

References

- Bica, E., Bonatto, C., & Dutra, C. M. 2003, *A&A*, 405, 991
- Binney, J., & Merrifield, M. 1998, *Galactic Dynamics*, Princeton Series in Astrophysics (Princeton: Princeton Univ. Press)
- Binney, J., & Tremaine, S. 1987, *Galactic Dynamics*, Princeton Series in Astrophysics (Princeton: Princeton Univ. Press)
- Bonatto, C., & Bica, E. 2003, *A&A*, 405, 525
- Bonatto, C., Bica, E., & Girardi, L. 2004, *A&A*, 415, 571
- Carpenter, J. M. 2001, *AJ*, 121, 2851
- Claria, J. J., & Lapasset, E. 1986, *AJ*, 91, 326
- Dutra, C. M., Santiago, B. X., & Bica, E. 2002, *A&A*, 381, 219
- Fiorucci, M., & Munari, U. 2003, *A&A*, 401, 781
- Jeffries, R. D., Thurston, M. R., & Hambly, N. C. 2001, *A&A*, 375, 863
- King, I. R. 1966, *AJ*, 71, 64
- Maciejewski, G., & Niedzielski, A. 2007, *A&A*, 467, 1065
- Marigo, P., Girardi, L., Bressan, A., et al. 2008, *A&A*, 482, 883
- Monet, D. G., Levine, S. E., Canzian, B., et al. 2003, *AJ*, 125, 984
- Nilakshi, Sagar, R., Pandey, A. K., & Mohan, V. 2002, *A&A*, 383, 153
- Roeser, S., Demleitner, M., & Schilbach, E. 2010, *AJ*, 139, 2440
- Salpeter, E. E. 1955, *ApJ*, 121, 161
- Scalo, J. 1998, in *Astronomical Society of the Pacific Conference Series 142, The Stellar Initial Mass Function (38th Herstmonceux Conference)*, eds. G. Gilmore, & D. Howell, 201
- Schlegel, D. J., Finkbeiner, D. P., & Davis, M. 1998, *ApJ*, 500, 525
- Sharma, S., Pandey, A. K., Ogura, K., et al. 2006, *AJ*, 132, 1669
- Skrutskie, M. F., Cutri, R. M., Stiening, R., et al. 2006, *AJ*, 131, 1163
- Tadross, A. L. 2011, *Journal of Korean Astronomical Society*, 44, 1